



Review

# Light-Triggered Formation of Surface Topographies in Azo Polymers

Matthew Hendrikx<sup>1,2</sup> , Albertus P. H. J. Schenning<sup>1,2</sup> , Michael G. Debije<sup>1</sup> and Dirk J. Broer<sup>1,2,\*</sup>

<sup>1</sup> Functional Organic Materials and Devices, Department of Chemical Engineering and Chemistry, Eindhoven University of Technology, 5612 AE Eindhoven, The Netherlands; M.Hendrikx@tue.nl (M.H.); A.P.H.J.Schenning@tue.nl (A.P.H.J.S.); M.G.Debije@tue.nl (M.G.D.)

<sup>2</sup> Institute for Complex Molecular Systems, Eindhoven University of Technology, P.O. Box 513, 5600 MB Eindhoven, The Netherlands

\* Correspondence: D.Broer@tue.nl

Academic Editor: Charles Rosenblatt

Received: 5 July 2017; Accepted: 22 July 2017; Published: 26 July 2017

**Abstract:** Properties such as friction, wettability and visual impact of polymer coatings are influenced by the surface topography. Therefore, control of the surface structure is of eminent importance to tuning its function. Photochromic azobenzene-containing polymers are an appealing class of coatings of which the surface topography is controllable by light. The topographies form without the use of a solvent, and can be designed to remain static or have dynamic properties, that is, be capable of reversibly switching between different states. The topographical changes can be induced by using linear azo polymers to produce surface-relief gratings. With the ability to address specific regions, interference patterns can imprint a variety of structures. These topographies can be used for nanopatterning, lithography or diffractive optics. For cross-linked polymer networks containing azobenzene moieties, the coatings can form topographies that disappear as soon as the light trigger is switched off. This allows the use of topography-forming coatings in a wide range of applications, ranging from optics to self-cleaning, robotics or haptics.

**Keywords:** azobenzene; surface topographies; surface relief gratings; liquid crystal networks; azo polymers; light responsive polymer coatings

## 1. Introduction

The surface of a material governs its contacts with its environment. Natural surfaces often allow for multiple functions, either to maintain a healthy living organism or simply to attract other organisms in order to procreate. A beautiful example of maintaining a healthy environment via a clean surface is the Lotus leaf [1]. This self-cleaning property relies on the nano- and micro-structuring of the leaf surface [2]. Multiple efforts have been made in creating artificial surfaces with functional properties inspired by nature [3]. An important strategy to functionalize a surface is to apply dimension-controlled elevations; that is, topographies. Outside nature-inspired applications, textured surfaces show promising optical properties, both as transmissive and reflective diffraction gratings [4,5]. Designing topographies on a surface can lead to applications in photonics (such as nanostructured polarizers and/or wave plates [6,7] and antireflection coatings [8–11]), friction control (including robotic fingerprints [12,13]), (de)wetting of surfaces and even control over cellular adhesion and mobility [14].

Surface topographies and reliefs can be created in multiple ways, either by physically imprinting (embossing [15,16]) or by manipulation of the material itself using light, temperature, pH, and/or solvent-swelling. Interestingly, light allows for a remote, contactless approach without changing the chemical environment. This contactless approach grants the possibility of locally

addressing and changing a material's surface/bulk properties (including shape [17–21], roughness and wettability [22,23], color [22,24], etc.). In order to make materials responsive to light, a light-sensitive molecule can be incorporated in the polymer [22]. A tremendous number of light-responsive trigger molecules exist [25]. One class of the most commonly used molecules is azobenzenes, first discovered in 1937 [26]. These molecules can undergo a reversible *trans*- and *cis*-isomerization induced by illumination (Figure 1a). For the most common azobenzene molecules, ultraviolet light irradiation induces the isomerization from *trans*-to-*cis*, while the reverse takes place via thermal relaxations or upon irradiation by visible light. Photoisomerization of azobenzene results in a large change of the molecular geometry, where the *trans*-isomer decreases in length between the *para*-carbon atoms from 10 to 6 Å. In turn, this results in a tremendous nanoscale force [27,28]. Moreover, this geometrical change between *trans*- and *cis*-isomer also leads to a change in dipole moment from near 0 to 3 Debye, for the *trans* and *cis* states, respectively [29,30]. These large geometrical changes make azobenzene one of the most interesting embeddable light-trigger molecules. Additionally, azobenzene molecules show dichroism, that is, higher absorption of polarized light along one axis compared to the orthogonal axis. This dichroic property induces a realignment orthogonal to the polarization direction of the incident light. This process is called 'photo-alignment' [31,32].

The design of topographies in azo polymeric materials can be achieved through different techniques, either via a patterned laser treatment on homogeneous surfaces or by designing a heterogeneous surface prior to illumination. Mainly, these techniques result in two surface states: the initial flat, regular state and a final textured state. Solid, light induced surface structures can be made in both linear and cross-linked polymer network materials containing azobenzene molecules without the need of a solvent (Figure 1b). Azo-containing polymers can range from azo dye doped [33,34], to azo side-chain [35–37], to azo main-chain amorphous polymers, and even azo functionalized LC polymers. The interaction of the chromophore and the polymer skeletal structure determines the efficiency of the topography formation.

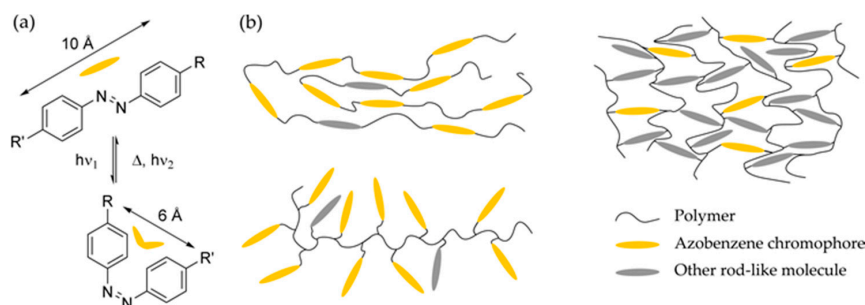


**Figure 1.** (a) Photo-isomerization of azobenzene; (b) Schematic representation of the azobenzene containing polymeric systems: linear polymers (top, left), side-chain polymers (bottom, left) and liquid crystal polymer networks (right).

In this review, the focus will be on surface relief gratings and topographies created by light in solid azobenzene-containing polymers. Light responsive coatings that contain other photochromic dyes (including spiropyrans or coumarins), gels, or hydrogels [22] are beyond the scope of this review. First, surface relief gratings based on linear azo polymers will be discussed and then topography changes in azo polymer networks will be presented.

## 2. Surface Relief Grating in Linear Azo Polymers

### 2.1. Light-Induced Permanent Surface Relief Gratings in Linear Azo Polymers

Soon after realizing the potential of azobenzene moieties in polymers to create surface patterns by illumination, the interest and development of these surface reliefs increased. In order to create surface structures with light, it is important to understand the influence of the azobenzene additive.

Both Natansohn and co-workers and Tripathy and co-workers simultaneously reported the formation of surface relief gratings (SRG) based on the photoisomerization of azobenzene [35,36]. For linear polymers containing this photosensitive molecule, it is necessary to incorporate the dye via (non-)covalent bonds to the polymer (via side or main chain or hydrogen bonding). By mere blending, or mixing, the interactions between the non-functionalized polymer and photosensitive azobenzenes are not sufficient to create and sustain the light induced patterns [38,39]. Moreover, the activation of the azobenzene molecule needs to be addressed in a specific order to cycle between *cis* and *trans* continuously [40]. One azobenzene derivative that is very interesting for this is Disperse Red 1, where visible light irradiation (488 nm) leads to continuous switching between *cis* and *trans* states. Upon incorporation of the acrylate derivative in a polymeric system by polymerization (Figure 2a), this continual switching is the driving force to the creation of SRGs upon irradiation with a laser interference pattern. In Figure 2b, a typical experimental setup is depicted to achieve a SRG in (an)isotropic materials. Exposure to interfering polarized light of appropriate wavelength led to an intensity interference pattern in the film, causing the exposed azobenzene derivatives to undergo isomerization reactions, leading to a realignment of the molecules. During this realignment, the azobenzene will preferentially align in a direction where the excitation is minimal. The resulting alignment of the *trans*-isomer will therefore be perpendicular to the direction of the electrical component of polarized light (Figure 2c). The realignment process is either powerful enough to move the polymer chains and/or fluidize the polymer, leading to the formation of an anisotropic fluid state [41]. It is known that during the light absorption of the azobenzene, localized heat is generated which can enable additional mobility [42]. This light-induced realignment process creates typical SRG topographies with the maxima located in the low intensity regions of the intensity interference pattern. This is observed for azo-containing polymers, even with high glass transition temperatures [43].

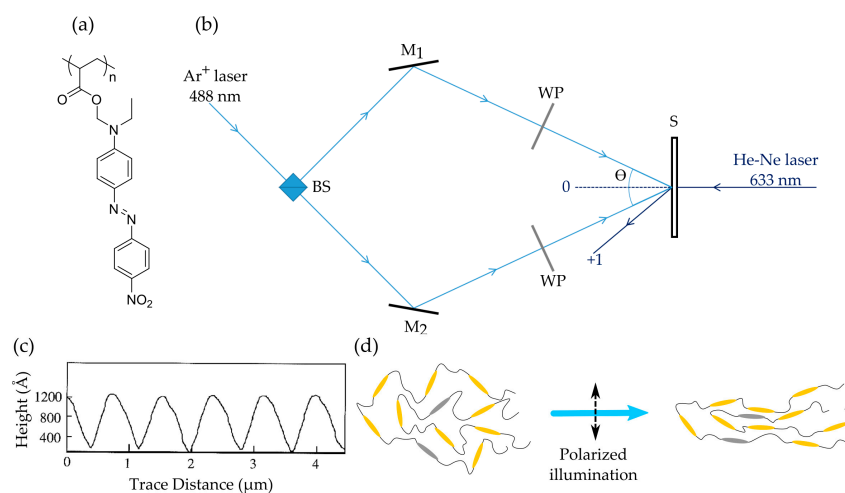


**Figure 2.** (a) Chemical structure of poly(Disperse Red 1 acrylate); (b) Experimental setup to write surface relief gratings in (an)isotropic azo-containing polymers. M<sub>1</sub>, M<sub>2</sub>: mirrors, BS: beamsplitter, WP: wave plate, S: azo-containing polymer,  $\theta$ : interference angle; (c) Typical AFM profile of a surface relief grating (SRG) topography. Reproduced from [36]; (d) The alignment of azo-containing polymers before and after polarized light illumination. The dashed line indicates the polarization direction of the light.

Different states of polarization are also used to fabricate gratings in azo polymer films. The polarization state can be out of the plane of incidence (s, senkrecht), in the plane of incidence (p, parallel) or even left- or right-hand circularly polarized (LCP and RCP, respectively). Normally, the use of s-s polarization geometry leads to weaker gratings, while the p-p, RCP-LCP geometry results in a much stronger and clearer pattern [44–47]. In contrast, research shows that the kinetics of the formation during the polarization sensitive lithography depend largely on the azo polymer's molecular weight [48]. Moreover, the content of the azo-based dye, the driving force of the formation

of the SRGs, determines the modulation depth that can be achieved by interference irradiation [49]. SRGs can be used for multiple applications, ranging from diffraction gratings, micro/nanostructuring, as molding templates, to etch masks. Priimagi and Shevchenko have previously summarized these photonic applications [47].

Generally, utilizing an azo polymer with the azo-chromophore covalently attached to the polymeric chain results in very stable and indelible SRGs. It is common for these materials to possess a high glass transition temperature,  $T_g$ , that leads to very stable gratings at temperatures below the glass transition; however, increasing the temperature above  $T_g$  typically results in removal of the grating [50]. Mostly the photosensitive azo dye remains photochemically stable after the thermal removal of the grating, leading to the possibility for rewritable applications. Furthermore, most SRGs do not show erasure during a second illumination below the glass transition. Utilizing azo dye-doped polymers [33,34], the gratings are not formed by migration of the polymer chain, but rather by the movement of the azobenzenes themselves, and the resulting structures are very weak. The first reported gratings [35,36] formed by azobenzene-containing polymers were side-chain azo polymers. These polymers have a high  $T_g$ , between 95 °C and 150 °C. Even with a  $T_g$  well above room temperature, these polymers showed gratings after exposure to interfering beams at room temperature. The topography of the SRG ranged between 100–200 nm and the efficiency was determined by the writing time. Most interestingly, Kim et al. showed in 1995 that orthogonal recording of two gratings leads to a two-dimensional grating. Stumpe and co-workers have shown that these higher dimensional gratings can also be fabricated from more easily accessible azo-containing polymers [51,52], leading even to colorless gratings via decoupling of the azobenzene after recording [51]. They achieved this by decomposing the urea group connecting the azobenzene to the polymeric chain. The azo polymer is based on poly[(phenyl isocyanate)-*co*-formaldehyde] and displayed in Figure 3a. However, the topography decreased from 600 nm to only 300 nm after decoupling. These gratings showed an extreme thermal stability, remaining even after heating to 300 °C. Moreover, using multilayered approaches, they were able to achieve three-dimensional gratings for more complex diffraction applications [53–55]. Coatings of an azobenzene-containing polyelectrolyte (PAZO, Figure 3b) of only 1.5  $\mu\text{m}$  thick showed topographies of 400 nm. Figure 3c,d depicts the systematic approach to achieving a multilayer 3D grating. This technique allows for the creation of hierarchical microstructures for new all-optical applications.

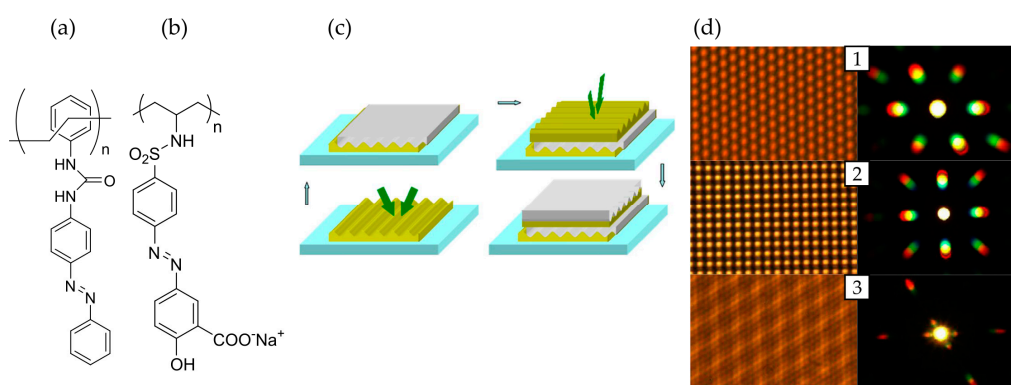


**Figure 3.** (a) Chemical structure of the azobenzene-urea polymer reported in reference [51]; (b) Chemical structure of the azobenzene-containing polyelectrolyte PAZO reported in reference [53–55]; (c) Schematic representation of the layer-by-layer fabrication of the 3D structures reported by Stumpe and co-workers; (d) Microscope and diffraction (Bertrand lens) images of hexagonal (1), tetragonal (2) and hierarchical (3) 3D structures. Reproduced from [55].

Goldenberg et al. used different cured epoxy resins containing azobenzenes to construct SRGs [52,56]. These epoxy resins allow for a solid state oxirane ring opening polymerization to achieve a polymer

film. This makes the synthesis of the polymeric species used for SRG fabrication more accessible and leads to an in-situ approach. Here, a ring opening reaction of bisphenol A diglycidyl ether and an azobenzene derivative was performed, leading to a covalent bond of the azobenzenes to the polymeric backbone (Figure 4a). These materials exhibit an extremely high inscription rate ( $0.45 \text{ min}^{-1}$ ) as well as a stable birefringence. This ‘inscription rate’ is defined by the ratio of the growing diffraction efficiency as a function of the inscription time [57]. The diffraction efficiency expresses the ratio of the power of the diffracted and the incident beam, respectively. The researchers showed that different ratios and variations of epoxy and azobenzene derivative lead to different inscription rates. Furthermore, these materials also allow for the creation of a tetragonal grating by two successive recordings.

Other techniques to create surface topographies by use of a polymeric system have been reported by Santer and co-workers [58]. In contrast to relying on the physical interactions between the polymeric species and the substrate, azo-functionalized polymer brushes were used (Figure 4c). These brushes were covalently bound to the substrate, resulting in degrafting upon irradiation with an interference pattern. This degrafting is a result of the accumulated stress in the polymer brushes as a result of the motion and relocation of the chromophores bound to the polymer (Figure 4d,e). The detached polymer can in turn move freely along the light intensity gradient, leaving the areas of origin to become thinner. Resulting topographies ranged from 5–60 nm. Depending on the distance of the light-induced mobility compared to the length of the polymer chains, the researchers produced SRGs that were either reversible or permanent after solvent treatment, dissolving and removing the broken-off polymer if degrafting occurred.

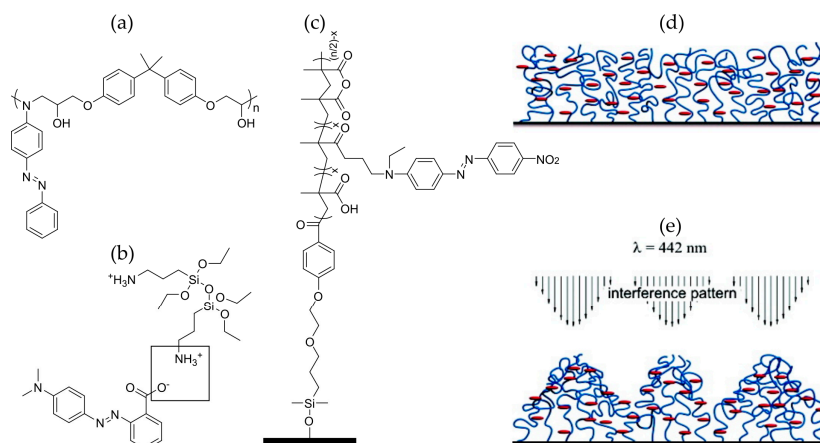


**Figure 4.** (a) Chemical structure of the polymer obtained by the oxirane ring opening reaction reported in reference [52,56]; (b) The chemical structure of complex formation obtained in the sol-gel material reported in reference [59]; (c) Chemical structure of the azo-functionalized poly(methacrylic acid) brush; (d,e) Schematic representation of the polymer brushes before (d) and after (e) interference pattern illumination. Note the polymer brushes create the maximum height in the low intensity region of the interference pattern. Reproduced from [58].

In contrast with these polymeric systems, SRGs can also be created via a sol-gel supramolecular approach [59]. This approach allows for easy production and the use of ionic interactions facilitates the dissolving of very high azo dye-doping concentrations without aggregation. This in turn leads to very effective formation of SRGs, as the azobenzenes and the polymeric chains show increased mobility due to these noncovalent interactions. The researchers dissolved different azobenzene derivatives in alkoxy silanes to achieve these SRGs. This formed an ionic matrix by noncovalent interactions, leading to an in-situ sol-gel reaction of alkoxy silane via condensation reaction (Figure 4b). These materials allowed for creation of gratings with a topography of 550 nm. Later, Stumpe and co-workers found that the grating formation when utilizing sol-gel techniques is greatly influenced by multiple factors such as cross-linking and plasticizing effects [60]. They also proposed a different ionic supramolecular



azobenzene-based material [61]. This ionic material allows for the creation of deep modulation depths (i.e., 1.8  $\mu\text{m}$ ) while being thermally stable up to 150  $^{\circ}\text{C}$  due to its strong ionic interactions. Furthermore, successive writings can be imprinted on the material, leading to conversion of a one-dimensional SRG into a two-dimensional SRG. This approach utilizing non-covalent links between the polymer chain and the chromophore has led to an increase in supramolecular approaches towards creating SRGs.

This supramolecular approach has also led to a better understanding in the creation of SRGs for s-s polarization configurations, shown by Sobolewska et al. [45,48], in which a hydrogen-bonded supramolecular polymer–azobenzene complex was used (P4VP(OH-DMA), Figure 5a). Depending on the molecular weight of the polymeric species, they achieved different diffraction efficiencies as a function of time. As depicted in Figure 5, for the s-s polarization configuration, it is important to utilize low molecular weight polymers. These smaller chains allow for better SRG formation and, in turn, better diffraction efficiencies. Interestingly, for the small chains, they found a secondary profile perpendicular to the grating wave-vector with modulation depth up to 200 nm (Figure 5b). The origin of this additional periodic topography is not clearly understood, but can be found in several examples [62–66]. Santer and co-workers have developed a method that allows in-situ atomic force microscopy during the formation of SRGs in azo-polymers. In their study [67], different SRGs were formed with different polarization geometries with an azo polymer electrolyte (see Figure 3b): this has led to a better understanding of the mechanism of SRG formation and the differences expressed during intensity and polarization interference irradiation. This work has proven that for intensity interference patterns, the topography maxima correspond to the position of intensity minima and vice versa (Figure 5d). Meanwhile, for the polarization interference pattern, they were able to reveal the topographic extremes and correlate them with the distribution of the  $\vec{E}$ -field vector within the polarization interference pattern. Here, the topographic maxima correspond to a “vertical”  $\vec{E}$ -field vector (Figure 5e). As seen in the graphs in Figure 5, the generation of surface topographies by light in azo-containing polymers is a slow process. These long time scales (10–60 min) preclude the use of such materials for applications requiring fast responses.

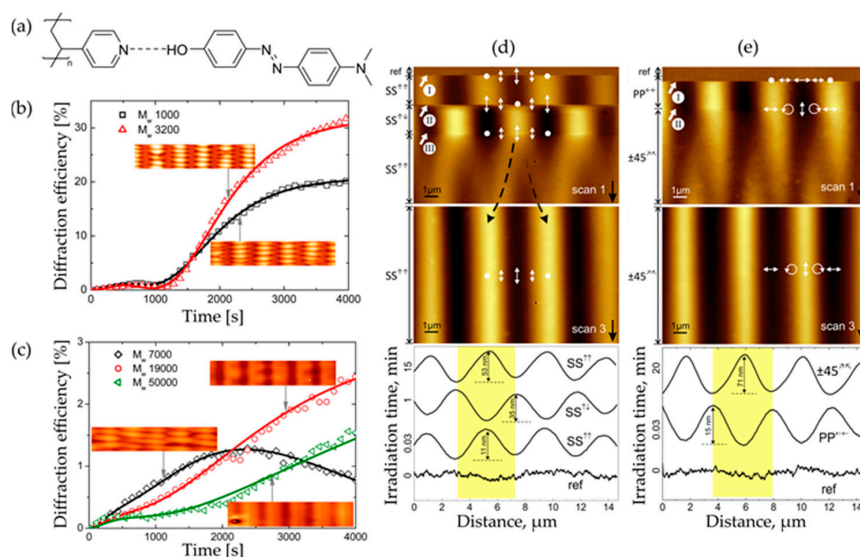


**Figure 5.** (a) Chemical structure of the hydrogen-bonded supramolecular azobenzene, P4VP(OH-DMA) complex; (b,c) Diffraction efficiency as a function of time using s-s polarization configuration for different molecular weights. Reproduced from [45]; (d) AFM micrographs and profile of the polymer topography with changing polarization state (depicted with white arrows) for intensity interference patterns and in-situ AFM recording; (e) AFM micrographs and profile of the polymer topography with changing interference pattern state for polarization interference pattern and in-situ AFM recording. Reproduced from [67].

Multiple research groups reported the construction of topographies in azo polymers using only one laser beam [65,68–71]. In all these works, the polarization state of the single laser beam is important in the generation of surface topographies. Tripathy et al. used Gaussian laser beams to write topographies in glassy azo polymers and noticed different shapes depending on the polarization state of the beam [69,72]. These illumination techniques generally led to the creation of craters, or single lines in the case of using a lens. Kucharski et al. investigated the generation of microgratings by positioning a liquid droplet on top of a 1 micron film and subsequently illuminating with a single coherent laser beam [70]. The microgratings ranged from 0.4–1.4  $\mu\text{m}$  in pitch with heights of approx. 100 nm, depending on the position under the droplet. Ambrosio and co-workers investigated the effect of illumination parameters on the spontaneous surface structuring in azo polymer films [65]. They focused a single coherent laser beam with a cylindrical or spherical lens resulting in local interference patterns. This led to the generation of a variety of topographies, ranging from gratings to dots, depending on the optical setup.

Even more structures can be made by use of evanescent surface plasmon fields [73,74]. As with SRGs, the intensity or polarization profile of the incoming light forms relief structures, necessarily diffraction limited. As described by Santer and co-workers, nanopatterned surface relief structures can be prepared by utilizing gold nanostructures to generate surface plasmon near fields upon ultraviolet irradiation [73]. Here, they positioned their supramolecular azobenzene–polymer complex on top of hexagonal Au-nanostructured array. Upon UV irradiation through the array while in-situ monitoring with AFM, the polymeric materials grow patterned topographies and the overall roughness of the surface increases over time. In contrast to temperature, increasing humidity removed these topographies. This method of creating surface topographies was further investigated by utilizing a silver nanoslit array [74]. This nanoslit approach is much more dependent on the wavelength and polarization of the incident light. Most importantly, topographical changes were only observed when the polarization direction was perpendicular to the slits. Utilizing a different wavelength led to a factor 3 decrease of the periodicity observed in the topographical pattern.

Researchers have used different azo chromophore loadings for the supramolecular polymer forming SRGs. Optimum degrees of loading between 50 and 75 mol % were determined, but these chromophore loading relationships are greatly dependent on the polymer used [43,75,76]. Most work focused on maximizing loading without losing grating efficiency. Koskela et al. [77] concentrated on achieving a lower limit of loading that still resulted in efficient gratings. Surprisingly, they reported that for their hydrogen bonded polymer (P4VP-OH(DMA)), only 1 mol % of chromophore loading was sufficient to obtain efficient gratings (Figure 5a); hence, the inscription rate is lowered by decreasing chromophore concentration. In addition to the use of hydrogen bonds to create supramolecular azobenzene-containing polymers, Priimagi and co-workers reported on the creation of supramolecular polymers by use of halogen bonds [78–81]. They determined the superiority of halogen-bonded polymer–azobenzene complexes over the analogous hydrogen-bonded complexes. The higher directionality of halogen bonding compared to hydrogen bonding allows fine-tuning of the polymer–chromophore interaction strength via single halogen atom mutation [78]. Furthermore, the use of halogen bonding allowed the creation of liquid crystalline complexes from non-mesogenic low molecular weight building blocks, in this case a stilbazole module. Moreover, the complex can be photoaligned by polarized light irradiation, resulting in a high degree of anisotropy (order parameter > 0.5). Additionally, this complex was able to create an efficient SRG upon irradiation with a RCP-LCP interference pattern with a modulation depth approximately 2.4 times the initial thickness of the film [79]. Recently, a more comparative study of different halogen bond donor chromophores showed that the efficiency of the SRG formation is increased with interaction strength (Figure 6). Moreover, the most effective halogen bond donor was found to be a iodoacetylene azo dye [81].

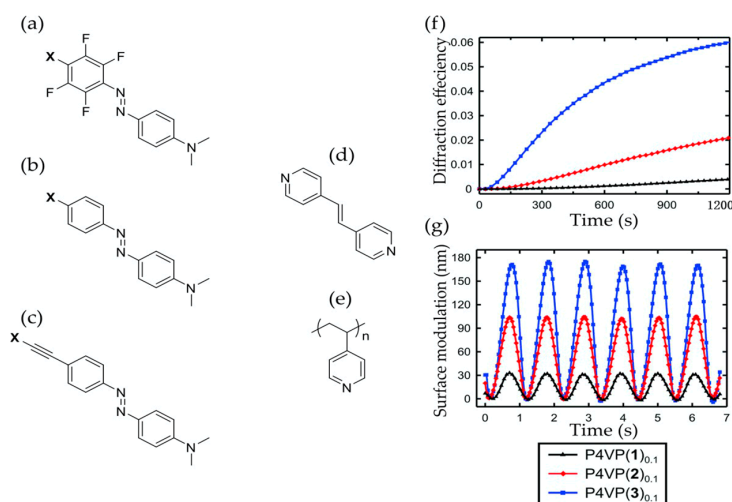


**Figure 6.** (a–e) Chemical structures of the different azobenzene modules (fluorinated (a), hydrogenated (b,c), dipyrindyl compound (d) and poly(4-vinyl pyridine) (P4VP, (e)) used in reference [81]. The label X can be either H, OH, or any halogen. (f) Diffraction efficiency of the different fluorinated and (g) AFM surface profiles of the gratings for azobenzene modules P4VP( $n$ )<sub>0.1</sub> (a) with  $n = 1$  (X = F),  $n = 2$  (X = Br) and  $n = 3$  (X = I). Reproduced from [81].

Seki et al. reported on liquid crystalline linear polymer systems that can create SRGs with light [38,82,83]. Moreover, they observed an enhancement in the SRG formation when using soft liquid crystalline azo polymers; they required a  $10^3$ -fold lower photon dose than for other common azobenzene polymers to complete the polymer migration. Remarkably, this migration occurred in the order of seconds. They found that pre-exposure with UV light generated *cis*-isomers which enhanced the photosensitivity of the liquid crystalline azo polymer [82,83]. They reported that using a supramolecular approach, the azobenzene unit can be detached with a consequent loss in topography height [38]. The same researchers reported cross-linking of the liquid crystal polymer after SRG formation increased the stability after heating [84]. Bobrovsky et al. investigated the creation of craters in amorphous, nematic and crystalline films of a bent-core compound containing azo polymer [71]. They observed that the material undergoes a fast transition from crystalline or nematic to isotropic upon UV light irradiation. They observed that the crater formation occurred only in thick nematic and cholesteric azo polymethacrylate polymer films (5–10  $\mu\text{m}$ ) [85]. For the nematic films, they found directional mass-transport along the LC-director.

Supramolecular main chain polymers can also be used to create SRGs. König et al. used a disk-shaped self-assembling molecule, consisting of three-arm azobenzene units to create effective gratings [86]. Interestingly, the resulting surface topography exceeds the films thickness prior to inscription. The surface topography formed reaches up to 350 nm for a 240 nm film. Depending on the molecular building block used, they could remove these gratings by heating above 120 °C, but also could generate gratings stable up to 260 °C.

## 2.2. Light-Induced Reversible Surface Relief Gratings in Linear Azo Polymers

A relief grating can undergo changes upon exposure to external triggers depending on the molecular weight of the polymer. Reducing the chain length of the polymer results in a decrease of the thermal stability of the grating, and above the  $T_g$  of the polymer, the grating grooves will diminish and disappear entirely, as discussed in Section 2.1. This section focuses on light-erasure of the gratings. Generally, a second flood illumination of circular or unpolarized light leads to the random alignment of embedded azo-chromophores. In turn, this leads to the partial or complete erasure of the SRGs. This light-initiated erasure of the gratings is more appealing than thermal erasure due to its capability of generating “on” and “off” states that can be controlled remotely, affect the film locally, and



on-demand. Numerous efforts have been made to remove gratings remotely by light, but generally have resulted in no or only partial erasure [34,65,87–89]. As described by Priimagi and co-workers, the ability to affect light-induced erasure seems to depend highly on the material's properties (including glass transition temperature, molecular weight, and so on) [90]. Unstable gratings formed utilizing polymers with low glass transition temperatures lead to eventual thermal self-erasure [83,91,92]. For these materials, the glass transition temperature is typically lower than ambient temperature. This leads to an unstable grating, which disappears over time, resulting in a flattened polymer coating in the dark and opening up possibilities of fabricating SRGs with temporal “on” and “off” states dictated by light exposure. In early efforts, Jiang et al. concluded that the erasure process is optimal when the erasing beam is polarized along the grating vector direction [87]. They investigated the erasure process by irradiating with a single polarized beam at normal incidence. They recorded gratings under different writing conditions (i.e., p-, s- and circular polarization), followed by erasure experiments with different polarization states than the writing beam (Figure 7a). However, they were unable to achieve full erasure and a topography of more than 10 nm remained after exposure. Ubukata and co-workers reported an erasure of 91% with a 3 nm remnant structure from a 35 nm deep SRG [88]. As mentioned earlier, Priimagi and co-workers found that the erasure capabilities of their supramolecular azobenzene–polymer complex (P4VP-OH(DMA), Figure 5a) is determined by its molecular weight and thus its glass transition temperature [90]. Notably, they reported that there is no polarization dependency in the erasure process of their P4VP–azobenzene complex in contrast to the results reported by Jiang et al. [87]. Moreover, the optical erasure was performed at least 30 °C below the  $T_g$  of the azobenzene–polymer complexes and still resulted in selective removal of the pattern. These azobenzene–polymer complexes allow for the writing and erasing of the SRG at room temperature, compared to the disadvantageous thermal erasure at high temperatures. Generally, the erasure process, or the ability to erase a SRG from a polymer coating, is expected to be related to the chemical structure, molecular weight, photo-orientation and photoinduced mechanical changes in the materials [90].

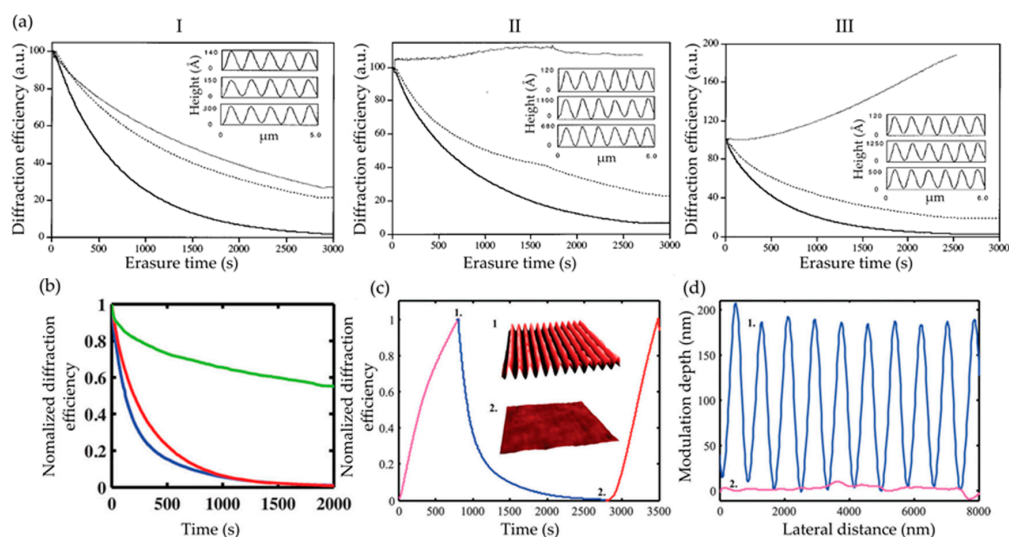


**Figure 7.** (a) The erasure behavior of SRGs under three erasing polarization conditions (parallel (solid) and perpendicular (dotted) polarized to the grating's grooves and circular (dashed) polarized light) with different writing conditions (I: p-p, II: s-s, III: circular polarized). Reproduced from [87]; (b) The erasure behavior of SRGs expressed as normalized diffraction efficiency for samples with molecular weights of 1000 (blue), 3200 (red) and 7000 (green)  $\text{g mol}^{-1}$ ; (c) Normalized diffraction efficiency of the SRG inscription (magenta), erasure (blue) and rewriting (red) of 1000  $\text{g mol}^{-1}$  azo-containing polymer. Insets show 3D AFM images of the inscribed (1) and erased SRG (2), with AFM surface profiles of these states shown in (d). Reproduced from [90].

Photo-shape memory is the polymer's ability to regain the initial shape imprinted by exposure to light. Kopyshv et al. [93] reported a photosensitive supramolecular polymer brush containing azobenzene (Figure 8a) attached to a substrate that, unlike the brushes described in Section 2.1, showed reversible changes in both thickness and roughness of the surface. With UV light exposure, the azobenzene–polymer brush complex shrinks and increases the roughness of the surface, while blue light irradiation causes the reverse effect. This material can form a chess board shaped SRG that alters its roughness and shape under UV irradiation, see Figure 8. They observed a photo-shape memory effect when irradiated with blue light, resulting in a smooth SRG.

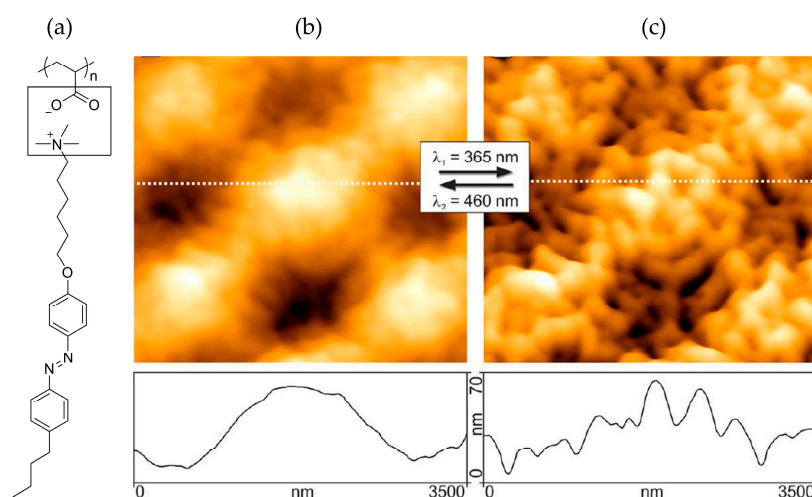


**Figure 8.** (a) Chemical structure of the supramolecular polymer brush used in reference [93]; (b,c) AFM micrographs of the in-situ recorded topography switching of a chessboard shaped SRG in a supramolecular azobenzene polymer brush complex during further UV irradiation (c) and after subsequent illumination with blue light (b). Reproduced from [93].

### 3. Surface Topographies in Cross-Linked Network Coatings

#### 3.1. Light-Induced Permanent Surface Topographies in Azo Cross-Linked Network Coatings

Permanent surface topographies have also been produced in polymer networks, and more specifically, in liquid crystal networks (LCN). LCs allow for a high degree of control over molecular alignment, which is important in forming topographies. LCNs are created from reactive LC monomeric mixtures that can be aligned by a variety of techniques (among them are various interfacial techniques, mechanical [14,94,95], optical [96–100] and electrical [101]). These mixtures typically contain an azobenzene moiety (molecule 4 in Figure 9c) acting both as a cross-linker and deformation trigger molecule. Once achieving the desired alignment, the monomeric mixture can be photopolymerized. Because of the average polyfunctionality of the chosen monomers, this leads to cross-linked liquid crystal polymer networks [102]. The ability to design and fabricate the anisotropic coating to respond to specific commands leads to the creation of many different directed topographies. Most interestingly, UV exposure of prealigned azo-containing LCN coatings induces the creation of topographies without the need of complex optical setups. Upon illumination, the azobenzene will undergo a *trans*-to-*cis* isomerization, leading to a disruption of the local molecular order. This results in expansion perpendicular and contraction parallel to the molecular alignment, known as the director  $\mathbf{n}$ , and thus leading to the creation of localized topographies when the coating has been pre-patterned via illumination through a mask. Figure 9 illustrates the expansion of the azo-LCN polymer coating and the principle of disruption in the alignment caused by the isomerization of the embedded azo molecule. Liu et al. have found that the topography formation is based on the creation of free volume inside the network. The free volume formation is enhanced by an azobenzene mesogen that also

acts as cross-linker [95,100,103]. Utilizing dual wavelength exposure, the azobenzene will undergo continuous *trans*–*cis*–*trans* photoisomerization that, in turn, leads to a maximum stress of the network, resulting in a larger surface topography [103].

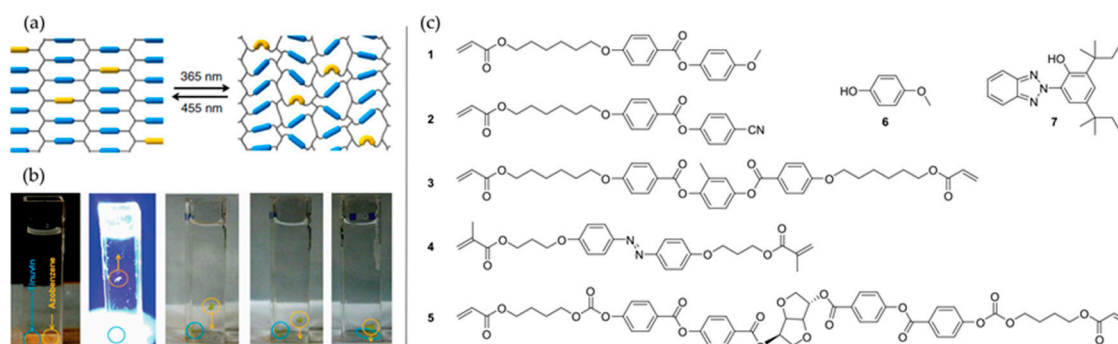


**Figure 9.** (a) The graphical representation of the polymeric network with copolymerized di-acrylate azobenzene with illumination of different wavelengths. Reproduced from [103]; (b) Density change in a chiral nematic polymer film containing copolymerized di-acrylate azobenzene (yellow circle) and the photoabsorber Tinuvin 328—molecule 7 above—(blue circle) before, during and after UV exposure in salt brine. Reproduced from [95]; (c) Chemical structures of the mixtures typically used to achieve glassy azo-liquid crystal networks (LCN) coatings. Molecules 1–3 make up the LCN, 4 is the azo crosslinker, 5 and 6 are a chiral dopant and radical scavenger, respectively, and 7 is a UV absorber.

In contrast to the formation of linear or amorphous polymer based SRGs, which require coherent light, incoherent light can create surface topographies in cross-linked, liquid crystal-based polymeric coatings. Interestingly, the methods for creating static or reversible LCN topographies are nearly identical. The difference lies in the chain length of the network. In contrast with SRGs, utilizing short chains forms stable topographies in cross-linked liquid crystalline polymer coatings, as this allows the chains to “fill” the free-volume generated during illumination, and additionally allows the azobenzene to rotate out of plane during the conversion from *cis*-to-*trans*. This rotation is only possible if the rotational mobility of the azobenzene in the LCN is sufficiently high [100].

By adding radical scavengers (molecule 6 in Figure 9c) to the mixture and controlling the polymerization of the coating, Liu et al. reported stable topography formation in azo-LCN coatings [95]. Here, they used a cross-linked cholesteric liquid crystal polymer coating, with regions selectively exposed through a mask with UV light: the chiral nematic (cholesteric) phase is present before and after UV exposure in Figure 10a. Cholesteric LC phases exhibit a reflection band determined by the pitch of the helical structure generated by the doping of the nematic LC with a chiral molecule; in this example, the center of the cholesteric reflection band is at 630 nm before UV exposure. Due to the disturbance of order of the network in the areas exposed to UV, the reflection band becomes narrower, as can be seen in the transmission spectra depicted in Figure 10b. The effective formation of topographies by actuation of the azobenzene is only present when exposing areas polymerized in the cholesteric phase. When using a coating instead polymerized in the isotropic phase, there is nearly no expression of topographies upon selective UV exposure: any topographies formed in the isotropic cross-linked coating result solely from thermal effects. Interestingly, when the azobenzene is swapped for a simple UV absorber, Tinuvin 328 (molecule 7 in Figure 9c), the topographies formed by selective illumination are lower in height than those generated using the azobenzene moiety (Figure 10c–f). Tinuvin 328 has an absorption spectrum that coincides with that of azobenzene [95]. However, Tinuvin 328 displays no large geometrical changes upon UV absorption as is observed for azobenzene. This leads the authors to conclude that the azobenzene isomerization is only partly responsible for the topographies, as thermally induced deformation from the absorbed UV light also plays a role. The cross-linked coatings

containing azobenzene show very stable topographies without observing any relaxation up to 120 °C, and persist for months when maintained at room temperature in the dark.

This technique was recently used to investigate cell adhesion and migration behavior to different sized surface topographies [14]. Here, UV irradiation of a planar cholesteric azo-LCN coating through a hexagonal dotted mask resulted in pillars. Depending on the dose of the UV illumination at a temperature above the  $T_g$ , different sized pillars were achieved by local expansion of the cholesteric coating. The resulting pillar-like topographies ranged from 0.2–1.6  $\mu\text{m}$ . The researchers used the pillar-structured coatings to study the interactions of living cells in contact with structured surfaces.

Stable topographies can also be prepared by locally controlling the alignment of the liquid crystal coating prior to polymerization and then generating the stable topographies in the film with uniform UV exposure after polymerization (that is, not using a mask as in the previous example) [13,100,101,104]. Stable topographies require the presence of radical scavengers during polymerization of the LC coating.

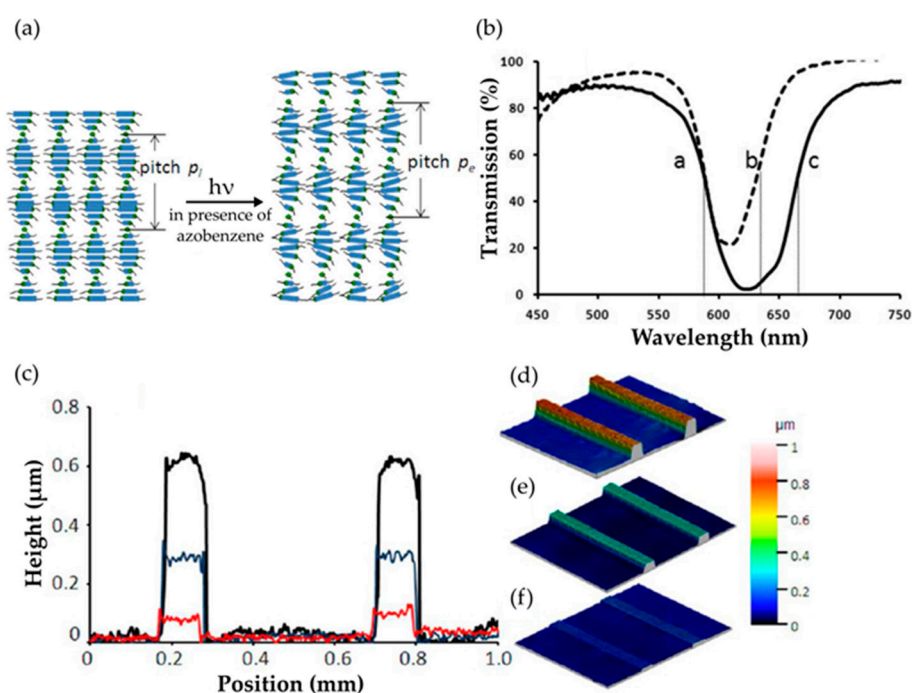


**Figure 10.** (a) Schematic representation of the cholesteric polymer coating before and after exposure with UV light with change in order; (b) Transmission spectra of the chiral nematic coating before (solid line) and after UV exposure (dashed line); (c) Surface profiles and the 3D view of the topographies made by masked UV exposure of the cholesteric polymer coating with azobenzene moiety (black line in (c,d)), Tinuvin 328 (blue line in (c,e)) and an isotropic coating with azobenzene (red line in (c,f)). Reproduced from [95].

McBride et al. used a different technique to create stable surface topographies in LCN materials. Topographies were formed relying on photoactivated reversible addition fragmentation chain transfer (RAFT)-based dynamic covalent chemistry in an azobenzene-free polymeric coating [105]. By implementing a chain transfer agent (CTA) inside the polymeric coating, the researchers could activate a nematic LCN coating through the CTA with a UV photoinitiator. When they carried out this process at elevated temperatures and addressed the coating with UV light exposing the film surface through a mask, the exposed areas of the LCN coating undergo a phase transition to isotropic, leading to a loss in order and concomitant increase in height. This in turn leads to the creation of surface topographies (400 nm) that are still present after cooling and subsequent heating.



### 3.2. Light-Induced Reversible Surface Topographies in Azo Cross-Linked Network Coatings

Reversible surface topographies can undergo a change after initial, under continuous, or during sequential illumination. In contrast with the permanent surface topographies, here the azo-LCN coating is prepared in the absence of any radical scavenger. This limits the mobility of the azobenzene under UV illumination, only allowing isomerization and the generation of disorder in the molecular alignment. This highly cross-linked azo-LCN coating can create topographies upon illumination, but the features are limited in stability. This results in a return to its initial state post-irradiation [100]. Liu et al. have proven that polymerization of a cholesteric-based film under the effects of localized electric fields creates azo-LCN coatings with alternating domains of planar (director parallel to the substrate) cholesteric and homeotropic (director perpendicular to the substrate) nematic alignment within the same film (see Figure 11a–c) [94,101]. With this alignment setup, the coating will contain areas that expand and contract in thickness adjacent to one another, resulting in larger differential topographical features. This makes the coating more attractive for applications such as generation of variable friction surfaces that can respond in the order of seconds (see Figure 11d,e).

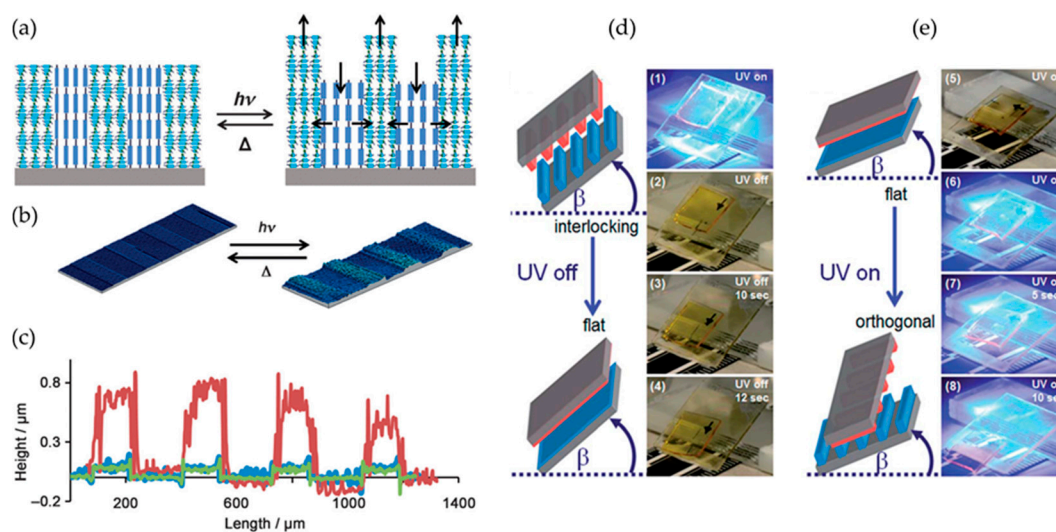


**Figure 11.** (a) Graphical illustration of the patterned coating with resulting influence of light; (b) 3D images of the coating in the absence and presence of light with different heights (c). Reproduced from [94]; (d,e) The slide-off of two pattern coated glass slides in contact and balanced at an angle  $\beta$  under the influence of UV light. The samples are positioned parallel (d) and orthogonal (e) with respect to one another, leading to different slide-off properties and friction. Reproduced from [101].

An example of surface topographies controlling friction was based on the self-assembly of cholesteric azo-LCN polymer coatings. Here, the cholesteric helical axis of the coating is aligned parallel to the substrate, leading to a so-called fingerprint texture [12]. The fingerprint texture is of particular interest as it contains multiple alignment regions (homeotropic and planar) directly upon application, and does not require additional electric fields or other processing states to achieve this condition. By containing both planar and homeotropic alignment regions in the same coating, the film will both expand and compress, respectively, leading to larger deformations [94,101]. For these types of azo-LCN coatings, it was found that the actuation and relaxation time were both close to 10 s [103]. The typical domain sizes achievable with azo-LCN coatings range from tens to hundreds of microns, with topographies varying between 0.1 and 2  $\mu\text{m}$ . It was also shown by experimental and computation results that self-assembled polydomain azo-LCN coatings could also generate films with light-switchable surface roughness [13].

Later, based on the materials reported by Liu et al., we performed further investigation on dynamic actuation that dispensed with the need to switch the triggering light on and off. The work



performed here [106] was inspired by the results found on the optical properties of azobenzenes in liquid crystal polymer films [107–109]. The dichroic properties of the azobenzene moiety allow for selective actuation of uniaxial aligned LCN domains. Here, two adjacent domains were orthogonally aligned via photoalignment, which employ polarized light and a polarization-sensitive alignment layer, by addressing the resulting deposited film with rotating linearly polarized UV light. This rotating polarized excitation light constantly changes the local photo-stationary state of the azo cross-linked network coating. We found continuous dynamic deformations located on and around the boundaries of the orthogonal aligned domains. Decreasing the domain sizes from 100  $\mu\text{m}$  to 20  $\mu\text{m}$  amplified the dynamic topographies and the corresponding oscillation. This change in size resulted in larger oscillations as visualized in Figure 12, although the frequency of the oscillation is slow (i.e., 0.014 Hz).

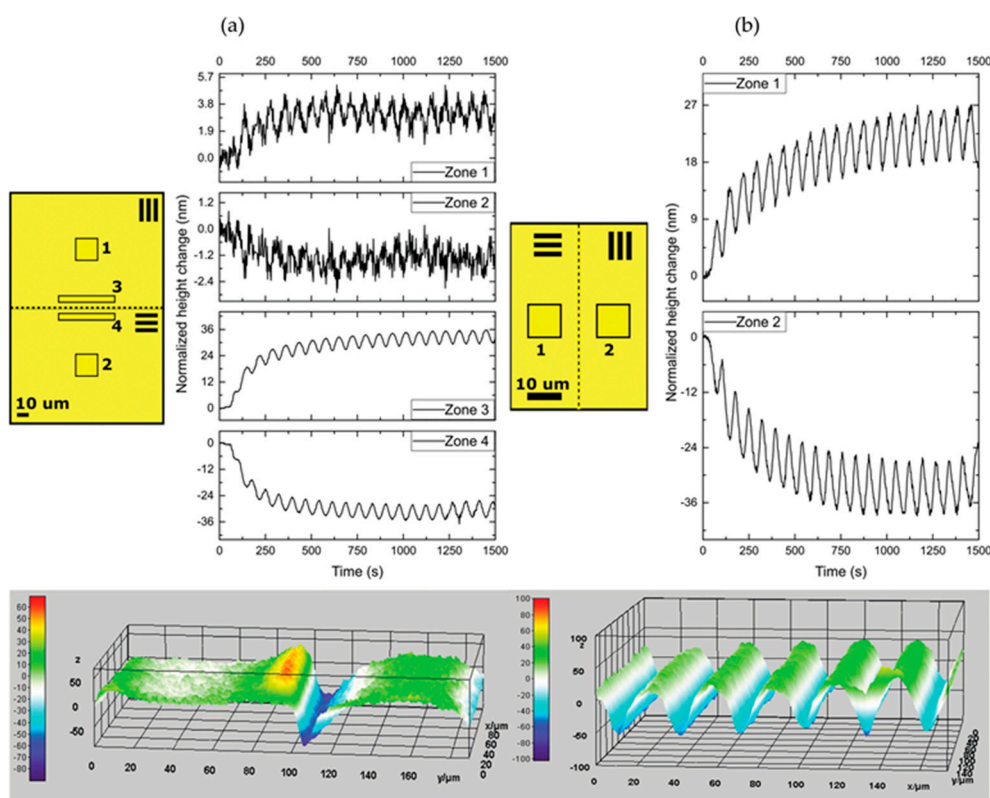


**Figure 12.** Oscillations and topographies observed in azo-LCN coatings aligned in orthogonal domains with sizes of 100  $\mu\text{m}$  (a) and 20  $\mu\text{m}$  (b) upon polarized light actuation. Topographies and their oscillations are located on and around the defect line. Reproduced from [106].

#### 4. Conclusions and Outlook

As can be concluded from this review, the generation of topographies in azobenzene polymer surfaces by light has been extensively researched. The use of light as a trigger to control the surface's structure has the advantage of being both contactless and able to affect the film remotely. Azobenzene containing polymers are highly suitable for creating topographies, and it is fascinating that these small, light-induced molecular shape changes can result in large amplified changes in the bulk polymeric material. Both for linear azo polymers as for azo cross-linked networks, this trigger molecule is able to create surface features. Typically, topography changes are larger in linear azo polymers as these polymers are more mobile. However, the reversibility of topographies is very limited (i.e., thermal or light erasure). To remove these stable topographies, high temperatures or short polymer chains are required. These processes are quite time-consuming. Azo cross-linked network coatings are

considerably faster in responding, and reversible topographies can be obtained easily. Moreover, so-called dynamic topographies can be achieved.

Future opportunities for light-induced structures on surfaces range from all-optical to more mechanical applications. In order to achieve a bright future, a deeper understanding of the light-induced processes is needed. The driving mechanism for the creation of topographies in both linear azo polymers and glassy LCN coatings remains controversial. For linear azo polymers, multiple mechanisms have been proposed [41]. Whereas with the azo polymer networks (azo-LCN), free volume generation in a glassy material seems to fit most of experimental data, this solution comes under question in light of the recent findings showing that also mechanical properties of the polymer network change upon illumination [110]. Recent research also shows an influence of temperature upon irradiation. This leads to photothermal effects described as photo-softening [42,110–112]. A full understanding of the driving mechanism in the creation of surface structures in azo polymers is sought to improve or fabricate new surface topography changing coatings.

The use of azobenzenes to achieve light-induced surface topographies comes with a downside. The typical absorption of azobenzene occurs at relatively short wavelengths. This limits the expected lifetime of the azo polymers, and in consequence, the potential of the host polymer. In addition, the position of the absorption bands of both the *trans* and *cis* state leads to typically yellow-colored coatings, which is often not desired. It has been shown that for specific linear azo polymers, this color can be removed, leading to permanent topographies [51]. Extensive research towards new applicable light triggered molecules [113] can lead to a more natural approach where the sun can be used as the light source [114]. The use of visible light triggering molecules (including azobenzenes) will continue to result in colored coatings. The slow kinetics of the azobenzene determine the speed of formation of surface topographies in azo polymers. Further research in faster responding systems has been performed for free-standing actuators and light-responsive molecules in solution [115].

With a better fundamental understanding and new chemistry, we foresee that light-induced surface topographies using azo polymers will find a large application space. Recent advances have already led to interesting applications outside the field of optics, especially for living cell adhesion and friction [14]. This work combined with the recent demonstration of dynamics and oscillations in surface topographies will lead the azobenzene-containing polymeric coatings in a new field of research.

**Acknowledgments:** This work was financially supported by the Netherlands Organization for Scientific Research (NWO–TOP PUNT Grant: 10018944), the European Research Council (Vibrate ERC, Grant 669991).

**Conflicts of Interest:** The authors declare no conflict of interest.

## References

1. Barthlott, W.; Neinhuis, C. Purity of the sacred lotus, or escape from contamination in biological surfaces. *Planta* **1997**, *202*, 1–8. [[CrossRef](#)]
2. Gorb, S.N. *Functional Surfaces in Biology*; Springer: New York, NY, USA, 2009; Volume 2.
3. Malshe, A.; Rajurkar, K.; Samant, A.; Hansen, H.N.; Bapat, S.; Jiang, W. Bio-inspired functional surfaces for advanced applications. *CIRP Ann. Manuf. Technol.* **2013**, *62*, 607–628. [[CrossRef](#)]
4. Kress, B.C.; Meyrueis, P. *Applied Digital Optics—From Micro Optics to Nanophotonics*; Wiley: Hoboken, NJ, USA, 2009.
5. Lohmüller, T.; Helgert, M.; Sundermann, M.; Brunner, R.; Spatz, J.P. Biomimetic interfaces for high-performance optics in the deep-UV light range. *Nano Lett.* **2008**, *8*, 1429–1433. [[CrossRef](#)] [[PubMed](#)]
6. Gansel, J.K.; Thiel, M.; Rill, M.S.; Decker, M.; Bade, K.; Saile, V.; von Freymann, G.; Linden, S.; Wegener, M. Gold helix photonic metamaterial as broadband circular polarizer. *Science* **2009**, *325*, 1513–1515. [[CrossRef](#)] [[PubMed](#)]
7. Pang, Y.; Gordon, R. Metal nano-grid reflective wave plate. *Opt. Express* **2009**, *17*, 2871. [[CrossRef](#)] [[PubMed](#)]
8. Chen, Q.; Hubbard, G.; Shields, P.A.; Liu, C.; Allsopp, D.W.E.; Wang, W.N.; Abbott, S. Broadband moth-eye antireflection coatings fabricated by low-cost nanoimprinting. *Appl. Phys. Lett.* **2009**, *94*, 263118. [[CrossRef](#)]

9. Morhard, C.; Pacholski, C.; Lehr, D.; Brunner, R.; Helgert, M.; Sundermann, M.; Spatz, J.P. Tailored antireflective biomimetic nanostructures for UV applications. *Nanotechnology* **2010**, *21*, 425301. [[CrossRef](#)] [[PubMed](#)]
10. Zhu, J.; Hsu, C.M.; Yu, Z.; Fan, S.; Cui, Y. Nanodome solar cells with efficient light management and self-cleaning. *Nano Lett.* **2010**, *10*, 1979–1984. [[CrossRef](#)] [[PubMed](#)]
11. Forberich, K.; Dennler, G.; Scharber, M.C.; Hingerl, K.; Fromherz, T.; Brabec, C.J. Performance improvement of organic solar cells with moth eye anti-reflection coating. *Thin Solid Films* **2008**, *516*, 7167–7170. [[CrossRef](#)]
12. Liu, D.; Broer, D.J. Self-assembled Dynamic 3D Fingerprints in Liquid-Crystal Coatings towards Controllable Friction and Adhesion. *Angew. Chem. Int. Ed.* **2014**, *126*, 4630–4634. [[CrossRef](#)]
13. Liu, D.; Liu, L.; Onck, P.R.; Broer, D.J. Reverse switching of surface roughness in a self-organized polydomain liquid crystal coating. *Proc. Natl. Acad. Sci. USA* **2015**, *112*, 3880–3885. [[CrossRef](#)] [[PubMed](#)]
14. Koçer, G.; ter Schiphorst, J.; Hendriks, M.; Kassa, H.G.; Leclère, P.; Schenning, A.P.H.J.; Jonkheijm, P. Light-Responsive Hierarchically Structured Liquid Crystal Polymer Networks for Harnessing Cell Adhesion and Migration. *Adv. Mater.* **2017**. [[CrossRef](#)] [[PubMed](#)]
15. Kommeren, S.; Sullivan, T.; Bastiaansen, C.W.M. Tunable surface topography in fluoropolymers using photo-embossing. *RSC Adv.* **2016**, *6*, 69117–69123. [[CrossRef](#)]
16. Adams, N.; De Gans, B.-J.; Kozodaev, D.; Sánchez, C.; Bastiaansen, C.W.M.; Broer, D.J.; Schubert, U.S. High-Throughput Screening and Optimization of Photoembossed Relief Structures. *J. Comb. Chem.* **2006**, *8*, 184–191. [[CrossRef](#)] [[PubMed](#)]
17. Van Oosten, C.L.; Bastiaansen, C.W.M.; Broer, D.J. Printed artificial cilia from liquid-crystal network actuators modularly driven by light. *Nat. Mater.* **2009**, *8*, 677–682. [[CrossRef](#)] [[PubMed](#)]
18. Lee, K.M.; Smith, M.L.; Koerner, H.; Tabiryan, N.; Vaia, R.A.; Bunning, T.J.; White, T.J. Photodriven, flexural-torsional oscillation of glassy azobenzene liquid crystal polymer networks. *Adv. Funct. Mater.* **2011**, *21*, 2913–2918. [[CrossRef](#)]
19. Gelebart, A.H.; Mc Bride, M.; Schenning, A.P.H.J.; Bowman, C.N.; Broer, D.J. Photoresponsive Fiber Array: Toward Mimicking the Collective Motion of Cilia for Transport Applications. *Adv. Funct. Mater.* **2016**, *26*, 5322–5327. [[CrossRef](#)]
20. White, T.J.; Tabiryan, N.V.; Serak, S.V.; Hrozhyk, U.A.; Tondiglia, V.P.; Koerner, H.; Vaia, R.A.; Bunning, T.J. A high frequency photodriven polymer oscillator. *Soft Matter* **2008**, *4*, 1796–1798. [[CrossRef](#)]
21. Van Oosten, C.L.; Corbett, D.; Davies, D.; Warner, M.; Bastiaansen, C.W.M.; Broer, D.J. Bending dynamics and directionality reversal in liquid crystal network photoactuators. *Macromolecules* **2008**, *41*, 8592–8596. [[CrossRef](#)]
22. Stumpel, J.E.; Broer, D.J.; Schenning, A.P.H.J. Stimuli-responsive photonic polymer coatings. *Chem. Commun.* **2014**, *50*, 15839–15848. [[CrossRef](#)] [[PubMed](#)]
23. Wagner, N.; Theato, P. Light-induced wettability changes on polymer surfaces. *Polymer* **2014**, *55*, 3436–3453. [[CrossRef](#)]
24. Brehmer, M.; Lub, J.; van der Witte, P. Light-induced color change of cholesteric copolymers. *Adv. Mater.* **1998**, *10*, 1438–1441. [[CrossRef](#)]
25. Abendroth, J.M.; Bushuyev, O.S.; Weiss, P.S.; Barrett, C.J. Controlling Motion at the Nanoscale: Rise of the Molecular Machines. *ACS Nano* **2015**, *9*, 7746–7768. [[CrossRef](#)] [[PubMed](#)]
26. Hartley, G.S. The *Cis*-form of Azobenzene. *Nature* **1937**, *140*, 281. [[CrossRef](#)]
27. Hugel, T. Single-Molecule Optomechanical Cycle. *Science* **2002**, *296*, 1103–1106. [[CrossRef](#)] [[PubMed](#)]
28. Holland, N.B.; Hugel, T.; Neuert, G.; Cattani-Scholz, A.; Renner, C.; Oesterheld, D.; Moroder, L.; Seitz, M.; Gaub, H.E. Single molecule force spectroscopy of azobenzene polymers: Switching elasticity of single photochromic macromolecules. *Macromolecules* **2003**, *36*, 2015–2023. [[CrossRef](#)]
29. Beharry, A.A.; Woolley, G.A. Azobenzene photoswitches for biomolecules. *Chem. Soc. Rev.* **2011**, *40*, 4422–4437. [[CrossRef](#)] [[PubMed](#)]
30. Fliegl, H.; Köhn, A.; Hättig, C.; Ahlrichs, R. Ab initio calculation of the vibrational and electronic spectra of trans- and cis-azobenzene. *J. Am. Chem. Soc.* **2003**, *125*, 9821–9827. [[CrossRef](#)] [[PubMed](#)]
31. Natansohn, A.; Rochon, P. Photoinduced motions in azo-containing polymers. *Chem. Rev.* **2002**, *102*, 4139–4175. [[CrossRef](#)] [[PubMed](#)]
32. Priimagi, A.; Barrett, C.J.; Shishido, A. Recent twists in photoactuation and photoalignment control. *J. Mater. Chem. C* **2014**, *2*, 7155–7162. [[CrossRef](#)]

33. Birabassov, R.; Landraud, N.; Galstyan, T.V.; Ritcey, A.; Bazuin, C.G.; Rahem, T. Thick dye-doped poly(methyl methacrylate) films for real-time holography. *Appl. Opt.* **1998**, *37*, 8264–8269. [[CrossRef](#)] [[PubMed](#)]
34. Labarthe, F.L.; Buffeteau, T.; Sourisseau, C. Analyses of the diffraction efficiencies, birefringence, and surface relief gratings on azobenzene-containing polymer films. *J. Phys. Chem. B* **1998**, *102*, 2654–2662. [[CrossRef](#)]
35. Rochon, P.; Batalla, E.; Natansohn, A. Optically induced surface gratings on azoaromatic polymer films. *Appl. Phys. Lett.* **1995**, *66*, 136–138. [[CrossRef](#)]
36. Kim, D.Y.; Tripathy, S.K.; Li, L.; Kumar, J. Laser-induced holographic surface relief gratings on nonlinear optical polymer films. *Appl. Phys. Lett.* **1995**, *66*, 1166–1168. [[CrossRef](#)]
37. Mandal, B.K.; Jeng, R.J.; Kumar, J.; Tripathy, S.K. New photocrosslinkable polymers for second-order nonlinear optical processes. *Die Makromol. Chem. Rapid Commun.* **1991**, *12*, 607–612. [[CrossRef](#)]
38. Zettsu, N.; Ogasawara, T.; Mizoshita, N.; Nagano, S.; Seki, T. Photo-triggered surface relief grating formation in supramolecular liquid crystalline polymer systems with detachable azobenzene units. *Adv. Mater.* **2008**, *20*, 516–521. [[CrossRef](#)]
39. Fiorini, C.; Prudhomme, N.; De Veyrac, G.; Maurin, I.; Raimond, P.; Nunzi, J.M. Molecular migration mechanism for laser induced surface relief grating formation. *Synth. Met.* **2000**, *115*, 121–125. [[CrossRef](#)]
40. Bandara, H.M.D.; Burdette, S.C. Photoisomerization in different classes of azobenzene. *Chem. Soc. Rev.* **2012**, *41*, 1809–1825. [[CrossRef](#)] [[PubMed](#)]
41. Yadavalli, N.S.; Loebner, S.; Papke, T.; Sava, E.; Hurduc, N.; Santer, S. A comparative study of photoinduced deformation in azobenzene containing polymer films. *Soft Matter* **2016**, *12*, 2593–2603. [[CrossRef](#)] [[PubMed](#)]
42. Vapaavuori, J.; Laventure, A.; Bazuin, C.G.; Lebel, O.; Pellerin, C. Submolecular Plasticization Induced by Photons in Azobenzene Materials. *J. Am. Chem. Soc.* **2015**, *137*, 13510–13517. [[CrossRef](#)] [[PubMed](#)]
43. Fukuda, T.; Matsuda, H.; Shiraga, T.; Kimura, T.; Kato, M.; Viswanathan, N.K.; Kumar, J.; Tripathy, S.K. Photofabrication of surface relief grating on films of azobenzene polymer with different dye functionalization. *Macromolecules* **2000**, *33*, 4220–4225. [[CrossRef](#)]
44. Viswanathan, N.K.; Balasubramanian, S.; Li, L.; Tripathy, S.K.; Kumar, J. A Detailed Investigation of the Polarization-Dependent Surface-Relief-Grating Formation Process on Azo Polymer Films. *Jpn. J. Appl. Phys.* **1999**, *38*, 5928–5937. [[CrossRef](#)]
45. Sobolewska, A.; Bartkiewicz, S.; Priimagi, A. High-Modulation-Depth Surface Relief Gratings Using s-s Polarization Configuration in Supramolecular Polymer—Azobenzene Complexes. *J. Phys. Chem. C* **2014**, *118*, 23279. [[CrossRef](#)]
46. Jiang, X.L.; Li, L.; Kumar, J.; Kim, D.Y.; Shivshankar, V.; Tripathy, S.K. Polarization dependent recordings of surface relief gratings on azobenzene containing polymer films. *Appl. Phys. Lett.* **1996**, *68*, 2618–2620. [[CrossRef](#)]
47. Priimagi, A.; Shevchenko, A. Azopolymer-based micro- and nanopatterning for photonic applications. *J. Polym. Sci. B Polym. Phys.* **2014**, *52*, 163–182. [[CrossRef](#)]
48. Sobolewska, A.; Bartkiewicz, S. Surface relief grating in azo-polymer obtained for s-s polarization configuration of the writing beams. *Appl. Phys. Lett.* **2012**, *101*, 193301. [[CrossRef](#)]
49. Vapaavuori, J.; Priimagi, A.; Kaivola, M. Photoinduced surface-relief gratings in films of supramolecular polymer-bisazobenzene complexes. *J. Mater. Chem.* **2010**, *20*, 5260–5264. [[CrossRef](#)]
50. Viswanathan, N.K.; Kim, D.Y.; Bian, S.; Williams, J.; Liu, W.; Li, L.; Samuelson, L.; Kumar, J.; Tripathy, S.K. Surface relief structures on azo polymer films. *J. Mater. Chem.* **1999**, *9*, 1941–1955. [[CrossRef](#)]
51. Goldenberg, L.M.; Kulikovskiy, L.; Kulikovska, O.; Stumpe, J.; Seki, T.; Ozaki, R.; Fujii, A.; Ozaki, M.; Kose, A. New materials with detachable azobenzene: Effective, colourless and extremely stable surface relief gratings. *J. Mater. Chem.* **2009**, *19*, 8068–8071. [[CrossRef](#)]
52. Goldenberg, L.M.; Kulikovskiy, L.; Kulikovska, O.; Stumpe, J.; Boilot, J.-P.; Tripathy, S.K.; Fujii, A.; Ozaki, M.; Kose, A. Extremely high patterning efficiency in easily made azobenzene-containing polymer films. *J. Mater. Chem.* **2009**, *19*, 6103–6105. [[CrossRef](#)]
53. Goldenberg, L.M.; Kulikovska, O.; Stumpe, J. Thermally stable holographic surface relief gratings and switchable optical anisotropy in films of an azobenzene-containing polyelectrolyte. *Langmuir* **2005**, *21*, 4794–4796. [[CrossRef](#)] [[PubMed](#)]
54. Gritsai, Y.; Goldenberg, L.M.; Kulikovska, O.; Stumpe, J. 3D structures using surface relief gratings of azobenzene materials. *J. Opt. A Pure Appl. Opt.* **2008**, *10*, 125304. [[CrossRef](#)]



55. Goldenberg, L.M.; Gritsai, Y.; Kulikovska, O.; Stumpe, J. Three-dimensional planarized diffraction structures based on surface relief gratings in azobenzene materials. *Opt. Lett.* **2008**, *33*, 1309–1311. [[CrossRef](#)] [[PubMed](#)]
56. Goldenberg, L.M.; Kulikovsky, L.; Gritsai, Y.; Kulikovska, O.; Tomczyk, J.; Stumpe, J.; Fujii, A.; Ozaki, M.; Kose, A. Very efficient surface relief holographic materials based on azobenzene-containing epoxy resins cured in films. *J. Mater. Chem.* **2010**, *20*, 9161–9171. [[CrossRef](#)]
57. Wang, X. *Azo polymers. Synthesis, functions, and Applications*; Springer: Berlin/Heidelberg, Germany, 2017.
58. Schuh, C.; Lomadze, N.; Rhüe, J.; Kopyshev, A.; Santer, S. Photomechanical Degrafting of Azo-Functionalized Poly(methacrylic acid) (PMAA) Brushes. *J. Phys. Chem. B* **2011**, *115*, 10431–10438. [[CrossRef](#)] [[PubMed](#)]
59. Kulikovska, O.; Goldenberg, L.M.; Kulikovsky, L.; Stumpe, J. Smart ionic sol-gel-based azobenzene materials for optical generation of microstructures. *Chem. Mater.* **2008**, *20*, 3528–3534. [[CrossRef](#)]
60. Kulikovsky, L.; Kulikovska, O.; Goldenberg, L.M.; Stumpe, J. Phenomenology of photoinduced processes in the ionic sol-gel-based azobenzene materials. *ACS Appl. Mater. Interfaces* **2009**, *1*, 1739–1746. [[CrossRef](#)] [[PubMed](#)]
61. Kulikovska, O.; Goldenberg, L.M.; Stumpe, J. Supramolecular azobenzene-based materials for optical generation of microstructures. *Chem. Mater.* **2007**, *19*, 3343–3348. [[CrossRef](#)]
62. Hubert, C.; Fiorini-Debuisschert, C.; Rocha, L.; Raimond, P.; Nunzi, J.-M. Spontaneous photoinduced patterning of azo-dye polymer films: the facts. *J. Opt. Soc. Am. B* **2007**, *24*, 1839–1846. [[CrossRef](#)]
63. Lee, S.; Jeong, Y.-C.; Park, J.-K. Unusual surface reliefs from photoinduced creeping and aggregation behavior of azopolymer. *Appl. Phys. Lett.* **2008**, *93*, 31912. [[CrossRef](#)]
64. Wang, X.; Yin, J.; Wang, X. Self-Structured Surface Patterns on Epoxy-Based Azo Polymer Films Induced by Laser Light Irradiation. *Macromolecules* **2011**, *44*, 6856–6867. [[CrossRef](#)]
65. Ambrosio, A.; Girardo, S.; Camposeo, A.; Pisignano, D.; Maddalena, P. Controlling spontaneous surface structuring of azobenzene-containing polymers for large-scale nano-lithography of functional substrates. *Appl. Phys. Lett.* **2013**, *102*, 93102. [[CrossRef](#)]
66. Lee, S.; Shin, J.; Kang, H.S.; Lee, Y.-H.; Park, J.-K. Deterministic Nanotexturing by Directional Photofluidization Lithography. *Adv. Mater.* **2011**, *23*, 3244–3250. [[CrossRef](#)] [[PubMed](#)]
67. Yadavalli, N.S.; Santer, S. In-situ atomic force microscopy study of the mechanism of surface relief grating formation in photosensitive polymer films. *J. Appl. Phys.* **2013**, *113*, 224304. [[CrossRef](#)]
68. Hubert, C.; Fiorini-Debuisschert, C.; Maurin, I.; Nunzi, J.M.; Raimond, P. Spontaneous patterning of hexagonal structures in an AZO-polymer using light-controlled mass transport. *Adv. Mater.* **2002**, *14*, 729. [[CrossRef](#)]
69. Bian, S.; Li, L.; Kumar, J.; Kim, D.Y.; Williams, J.; Tripathy, S.K. Single laser beam-induced surface deformation on azobenzene polymer films. *Appl. Phys. Lett.* **1998**, *73*, 1817–1819. [[CrossRef](#)]
70. Barille, R.; Nunzi, J.M.; Ahmadi-Kandjani, S.; Ortyl, E.; Kucharski, S. One step inscription of surface relief microgratings. *Opt. Commun.* **2007**, *280*, 217–220. [[CrossRef](#)]
71. Bobrovsky, A.; Mochalov, K.; Oleinikov, V.; Solovyeva, D.; Shibaev, V.; Bogdanova, Y.; Hamplová, V.; Kašpar, M.; Bubnov, A. Photoinduced Changes of Surface Topography in Amorphous, Liquid-Crystalline, and Crystalline Films of Bent-Core Azobenzene-Containing Substance. *J. Phys. Chem. B* **2016**, *120*, 5073–5082. [[CrossRef](#)] [[PubMed](#)]
72. Bian, S.; Liu, W.; Williams, J.; Samuelson, L.; Kumar, J.; Tripathy, S. Photoinduced surface relief grating on amorphous poly(4-phenylazophenol) films. *Chem. Mater.* **2000**, *12*, 1585–1590. [[CrossRef](#)]
73. König, T.; Goldenberg, L.M.; Kulikovska, O.; Kulikovsky, L.; Stumpe, J.; Santer, S. Reversible structuring of photosensitive polymer films by surface plasmon near field radiation. *Soft Matter* **2011**, *7*, 4174–4178. [[CrossRef](#)]
74. König, T.; Tsukruk, V.V.; Santer, S. Controlled topography change of subdiffraction structures based on photosensitive polymer films induced by surface plasmon polaritons. *ACS Appl. Mater. Interfaces* **2013**, *5*, 6009–6016. [[CrossRef](#)] [[PubMed](#)]
75. Andruzzi, L.; Altomare, A.; Ciardelli, F.; Solaro, R.; Hvilsted, S.; Ramanujam, P.S. Holographic gratings in azobenzene side-chain polymethacrylates. *Macromolecules* **1999**, *32*, 448–454. [[CrossRef](#)]
76. Börger, V.; Kulikovska, O.; G-Hubmann, K.; Stumpe, J.; Huber, M.; Menzel, H. Novel polymers to study the influence of the azobenzene content on the photo-induced surface relief grating formation. *Macromol. Chem. Phys.* **2005**, *206*, 1488–1496. [[CrossRef](#)]



77. Koskela, J.E.; Vapaavuori, J.; Ras, R.H.A.; Priimagi, A. Light-Driven Surface Patterning of Supramolecular Polymers with Extremely Low Concentration of Photoactive Molecules. *ACS Macro Lett.* **2014**, *3*, 1196–1200. [[CrossRef](#)]
78. Priimagi, A.; Cavallo, G.; Forni, A.; Gorynsztein-Leben, M.; Kaivola, M.; Metrangolo, P.; Milani, R.; Shishido, A.; Pilati, T.; Resnati, G.; et al. Photoresponsive Supramolecular Polymers: Halogen Bonding versus Hydrogen Bonding in Driving Self-Assembly and Performance of Light-Responsive Supramolecular Polymers. *Adv. Funct. Mater.* **2012**, *22*, 2571. [[CrossRef](#)]
79. Priimagi, A.; Saccone, M.; Cavallo, G.; Shishido, A.; Pilati, T.; Metrangolo, P.; Resnati, G. Photoalignment and Surface-Relief-Grating Formation are Efficiently Combined in Low-Molecular-Weight Halogen-Bonded Complexes. *Adv. Mater.* **2012**, *24*, OP345–OP352. [[CrossRef](#)] [[PubMed](#)]
80. Priimagi, A.; Cavallo, G.; Metrangolo, P.; Resnati, G. The Halogen Bond in the Design of Functional Supramolecular Materials: Recent Advances. *Acc. Chem. Res.* **2013**, *46*, 2686–2695. [[CrossRef](#)] [[PubMed](#)]
81. Saccone, M.; Dichiarante, V.; Forni, A.; Goulet-Hanssens, A.; Cavallo, G.; Vapaavuori, J.; Terraneo, G.; Barrett, C.J.; Resnati, G.; Metrangolo, P.; et al. Supramolecular hierarchy among halogen and hydrogen bond donors in light-induced surface patterning. *J. Mater. Chem. C* **2015**, *3*, 759–768. [[CrossRef](#)]
82. Zettsu, N.; Ogasawara, T.; Arakawa, R.; Nagano, S.; Ubukata, T.; Seki, T. Highly photosensitive surface relief gratings formation in a liquid crystalline azobenzene polymer: New implications for the migration process. *Macromolecules* **2007**, *40*, 4607–4613. [[CrossRef](#)]
83. Zettsu, N.; Seki, T. Highly efficient photogeneration of surface relief structure and its immobilization in cross-linkable liquid crystalline azobenzene polymers. *Macromolecules* **2004**, *37*, 8692–8698. [[CrossRef](#)]
84. Zettsu, N.; Ubukata, T.; Seki, T.; Ichimura, K. Soft crosslinkable azo polymer for rapid surface relief formation and persistent fixation. *Adv. Mater.* **2001**, *13*, 1693–1697. [[CrossRef](#)]
85. Bobrovsky, A.; Mochalov, K.; Chistyakov, A.; Oleinikov, V.; Shibaev, V. AFM study of laser-induced crater formation in films of azobenzene-containing photochromic nematic polymer and cholesteric mixture. *J. Photochem. Photobiol. A Chem.* **2014**, *275*, 30–36. [[CrossRef](#)]
86. Goldenberg, L.M.; Kulikovskiy, L.; Kulikovskaya, O.; Tomczyk, J.; Stumpe, J. Thin Layers of Low Molecular Azobenzene Materials with Effective Light-Induced Mass Transport. *Langmuir* **2010**, *26*, 2214–2217. [[CrossRef](#)] [[PubMed](#)]
87. Jiang, X.L.; Li, L.; Kumar, J.; Kim, D.Y.; Tripathy, S.K. Unusual polarization dependent optical erasure of surface relief gratings on azobenzene polymer films. *Appl. Phys. Lett.* **1998**, *72*, 2502–2504. [[CrossRef](#)]
88. Ubukata, T.; Isoshima, T.; Hara, M. Wavelength-Programmable Organic Distributed-Feedback Laser Based on a Photoassisted Polymer-Migration System. *Adv. Mater.* **2005**, *17*, 1630–1633. [[CrossRef](#)]
89. Barrett, C.J.; Natansohn, A.L.; Rochon, P.L. Mechanism of Optically Inscribed High-Efficiency Diffraction Gratings in Azo Polymer Films. *J. Phys. Chem.* **1996**, *100*, 8836–8842. [[CrossRef](#)]
90. Vapaavuori, J.; Ras, R.H.A.; Kaivola, M.; Bazuin, C.G.; Priimagi, A. From partial to complete optical erasure of azobenzene–polymer gratings: Effect of molecular weight. *J. Mater. Chem. C* **2015**, *3*, 11011–11016. [[CrossRef](#)]
91. Luca, A.R.; Moleavin, I.-A.; Hurduc, N.; Hamel, M.; Rocha, L. Mass transport in low Tg azo-polymers: Effect on the surface relief grating induction and stability of additional side chain groups able to generate physical interactions. *Appl. Surf. Sci.* **2014**, *290*, 172–179. [[CrossRef](#)]
92. Isayama, J.; Nagano, S.; Seki, T. Phototriggered Mass Migrating Motions in Liquid Crystalline Azobenzene Polymer Films with Systematically Varied Thermal Properties. *Macromolecules* **2010**, *43*, 4105–4112. [[CrossRef](#)]
93. Kopyshchev, A.; Galvin, C.J.; Patil, R.R.; Genzer, J.; Lomadze, N.; Feldmann, D.; Zakrevski, J.; Santer, S. Light-Induced Reversible Change of Roughness and Thickness of Photosensitive Polymer Brushes. *ACS Appl. Mater. Interfaces* **2016**, *8*, 19175–19184. [[CrossRef](#)] [[PubMed](#)]
94. Liu, D.; Bastiaansen, C.W.M.; den Toonder, J.M.J.; Broer, D.J. Photo-Switchable Surface Topologies in Chiral Nematic Coatings. *Angew. Chem. Int. Ed.* **2012**, *51*, 892–896. [[CrossRef](#)] [[PubMed](#)]
95. Liu, D.; Bastiaansen, C.W.M.; den Toonder, J.M.J.; Broer, D.J. Light-induced formation of dynamic and permanent surface topologies in chiral-nematic polymer networks. *Macromolecules* **2012**, *45*, 8005–8012. [[CrossRef](#)]
96. McConney, M.E.; Martinez, A.; Tondiglia, V.P.; Lee, K.M.; Langley, D.; Smalyukh, I.I.; White, T.J. Topography from topology: Photoinduced surface features generated in liquid crystal polymer networks. *Adv. Mater.* **2013**, *25*, 5880–5885. [[CrossRef](#)] [[PubMed](#)]

97. Ahn, S.; Ware, T.H.; Lee, K.M.; Tondiglia, V.P.; White, T.J. Photoinduced Topographical Feature Development in Blueprinted Azobenzene-Functionalized Liquid Crystalline Elastomers. *Adv. Funct. Mater.* **2016**, *26*, 5819–5826. [[CrossRef](#)]
98. De Haan, L.T.; Leclère, P.; Damman, P.; Schenning, A.P.H.J.; Debije, M.G. On-demand wrinkling patterns in thin metal films generated from self-assembling liquid crystals. *Adv. Funct. Mater.* **2015**, *25*, 1360–1365. [[CrossRef](#)]
99. De Haan, L.T.; Sánchez-Somolinos, C.; Bastiaansen, C.M.W.; Schenning, A.P.H.J.; Broer, D.J. Engineering of Complex Order and the Macroscopic Deformation of Liquid Crystal Polymer Networks. *Angew. Chem. Int. Ed.* **2012**, *51*, 12469–12472. [[CrossRef](#)] [[PubMed](#)]
100. Liu, D.; Broer, D.J. Liquid crystal polymer networks: switchable surface topographies. *Liq. Cryst. Rev.* **2013**, *1*, 20–28. [[CrossRef](#)]
101. Liu, D.; Broer, D.J. Light controlled friction at a liquid crystal polymer coating with switchable patterning. *Soft Matter* **2014**, *10*, 7952–7958. [[CrossRef](#)] [[PubMed](#)]
102. Liu, D.; Broer, D.J. Liquid crystal polymer networks: Preparation, properties, and applications of films with patterned molecular alignment. *Langmuir* **2014**, *30*, 13499–13509. [[CrossRef](#)] [[PubMed](#)]
103. Liu, D.; Broer, D.J. New insights into photoactivated volume generation boost surface morphing in liquid crystal coatings. *Nat. Commun.* **2015**, *6*, 8334. [[CrossRef](#)] [[PubMed](#)]
104. Liu, D.; van Oosten, C.; Bastiaansen, C.W.M.; Broer, D.J. Photoresponsive Liquid Crystalline Polymeric Materials. *Adapt. Act. Multifunct. Smart Mater. Syst.* **2013**, *77*, 325–332. [[CrossRef](#)]
105. McBride, M.K.; Hendriks, M.; Liu, D.; Worrell, B.T.; Broer, D.J.; Bowman, C.N. Photoinduced Plasticity in Cross-Linked Liquid Crystalline Networks. *Adv. Mater.* **2017**. [[CrossRef](#)] [[PubMed](#)]
106. Hendriks, M.; Schenning, A.; Broer, D.J. Patterned oscillating topographical changes in photoresponsive polymer coatings. *Soft Matter* **2017**, *13*, 4321–4327. [[CrossRef](#)] [[PubMed](#)]
107. Yu, Y.; Nakano, M.; Ikeda, T. Directed bending of a polymer film by light. *Nature* **2003**, *425*, 145. [[CrossRef](#)] [[PubMed](#)]
108. White, T.J.; Serak, S.V.; Tabiryian, N.V.; Vaia, R.A.; Bunning, T.J. Polarization-controlled, photodriven bending in monodomain liquid crystal elastomer cantilevers. *J. Mater. Chem.* **2009**, *19*, 1080–1085. [[CrossRef](#)]
109. Smith, M.L.; Lee, K.M.; White, T.J.; Vaia, R.A. Design of polarization-dependent, flexural-torsional deformation in photo responsive liquid crystalline polymer networks. *Soft Matter* **2014**, *10*, 1400–1410. [[CrossRef](#)] [[PubMed](#)]
110. Kumar, K.; Schenning, A.; Broer, D.J.; Liu, D. Regulating the Modulus of a Chiral Liquid Crystal Polymer Network by Light. *Soft Matter* **2016**, *12*, 3196–3201. [[CrossRef](#)] [[PubMed](#)]
111. Harrison, J.M.; Goldbaum, D.; Corkery, T.C.; Barrett, C.J.; Chromik, R.R. Nanoindentation studies to separate thermal and optical effects in photo-softening of azo polymers. *J. Mater. Chem. C* **2015**, *3*, 995–1003. [[CrossRef](#)]
112. Gelebart, A.H.; Vantomme, G.; Meijer, B.E.W.; Broer, D.J. Mastering the Photothermal Effect in Liquid Crystal Networks: A General Approach for Self-Sustained Mechanical Oscillators. *Adv. Mater.* **2017**. [[CrossRef](#)] [[PubMed](#)]
113. Bléger, D.; Hecht, S. Visible-Light-Activated Molecular Switches. *Angew. Chem. Int. Ed.* **2015**, *54*, 11338–11349. [[CrossRef](#)] [[PubMed](#)]
114. Kumar, K.; Knie, C.; Bléger, D.; Peletier, M.A.; Friedrich, H.; Hecht, S.; Broer, D.J.; Debije, M.G.; Schenning, A.P.H.J. A chaotic self-oscillating sunlight-driven polymer actuator. *Nat. Commun.* **2016**, *7*, 11975. [[CrossRef](#)] [[PubMed](#)]
115. García-Amorós, J.; Velasco, D. Recent advances towards azobenzene-based lightdriven real-time information-transmitting materials. *Beilstein J. Org. Chem.* **2012**, *8*, 1003–1017. [[CrossRef](#)] [[PubMed](#)]

